Studying kidney injury using the Operetta High Content Imaging System: Analysis of the podocyte cytoskeleton on CYTOO micropatterns

Matthias Fassler[1], Kenneth Young[2], Stefan Jaeger[2], Gisela Abt[2], Olaf Deppe[1], Karin Boettcher[1]
[1] PerkinElmer Inc., [2] Evotec AG

1 Introduction

Drug-induced nephrotoxicity is one of the most frequent reasons for the failure of new chemical entities (NCEs) in clinical trials during drug development. It is now widely accepted that the podocyte is one of the key cell types affected by nephrotoxicity and kidney diseases such as diabetic nephropathy [Mathieson, 2012]. The podocyte is a highly differentiated epithelial cell type with a unique cytoskeletal architecture that forms small foot processes. This complex cytoskeleton is frequently damaged during kidney injury, thereby abrogating the filtration capacity of the kidney [Wang *et al*., 2012].

Here we present a high content screening application to analyze the integrity of the podocyte actin cytoskeleton. Using the Operetta® High Content Imaging System (PerkinElmer), we acquired images of podocytes grown on CYTOO chips™ and analyzed drug-induced changes in podocyte morphology using the Harmony® High Content Imaging and Analysis Software.

We demonstrate that CYTOO micropattern-based analysis of podocyte integrity on the Operetta system is a viable option to screen for complex cytoskeletal rearrangements.

2 Assay principle

Conditionally immortalized human podocytes were cultured as described in Saleem *et al.*, 2002. Cells were differentiated in RPMI-1640 containing 2% FCS for 10-14 days and then seeded onto CYTOO chips™ within a 6-well cell culture plate. We used L-shaped micropatterns with a size of 1600 µm² coated with red fluorescent Fibronectin (FN650). Cells of two different chips were either left untreated or were treated with 10 µM ROCK inhibitor Y-27632 prior to fixation with 4% paraformaldehyde. Cells were permeabilized and stained with Alexa Fluor® 488 Phalloidin and Hoechst. Stained CYTOO chips™ were then mounted onto microscope slides.

Using an Operetta system equipped with a slide holder and a 10X high NA objective, we acquired widefield images of the three channels. We measured 54 image fields in both the treated and untreated CYTOO chips™.

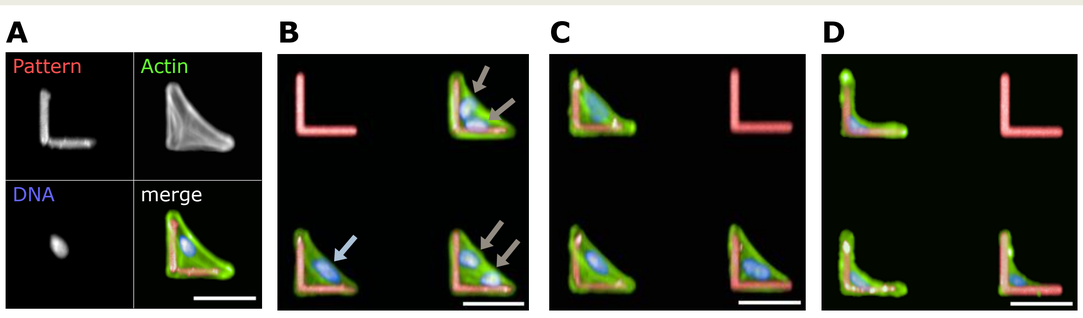

Figure 1. Podocytes grown on CYTOO micropatterns. A) Micrographs of a single podocyte grown on an L-shaped micropattern. B) Based on the nuclear staining, approximately 50% of the occupied micropatterns were occupied by more than one cell (dark grey arrows). For the analysis, we focused on isolated podocytes on micropatterns (light blue arrow). Overall, approximately 50% of the micropatterns were occupied by one or more podocytes. C) Untreated podocytes form a stress fiber between both arms of the micropattern and adopt a triangular shape. D) Podocytes treated with a ROCK inhibitor adopt an L-shape.

3 Micropattern statistics and cytoskeletal phenotype

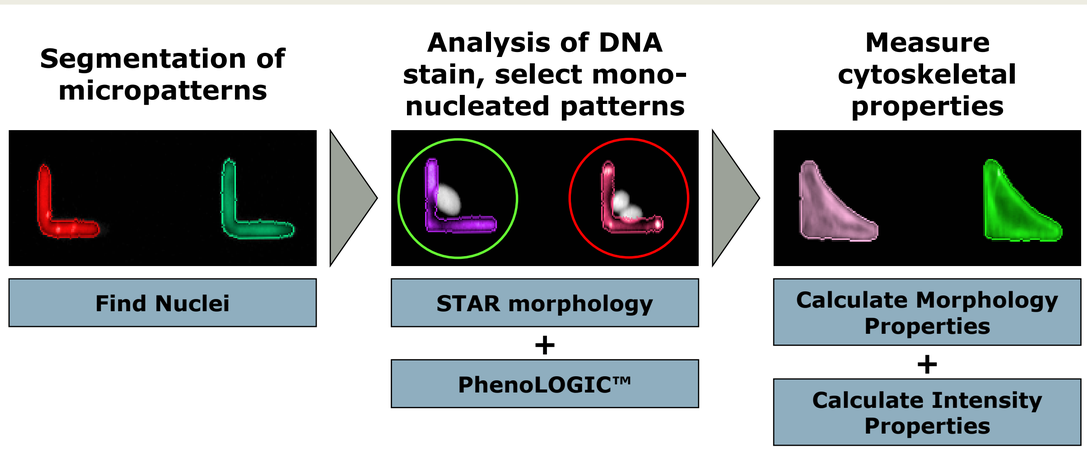

Figure 2. Outline of the image analysis strategy. Images were analyzed using the building blocks of the Harmony software. In the first step we segmented the image based on the staining of the micropatterns, using the building block *Find Nuclei* (tuned with an atypical set of parameters). Next, we identified the outline of the cells based on the Actin stain (not shown). To isolate mononucleated micropatterns, we analyzed the fluorescence distribution of the Hoechst stain using STAR morphology properties. Subsequently, we trained the PhenoLOGIC™ supervised machine learning algorithm (PerkinElmer) to distinguish between mono- and polynucleated patterns based on the STAR morphology properties. Lastly, we quantified the intensity and morphology properties of the podocyte cytoskeleton.

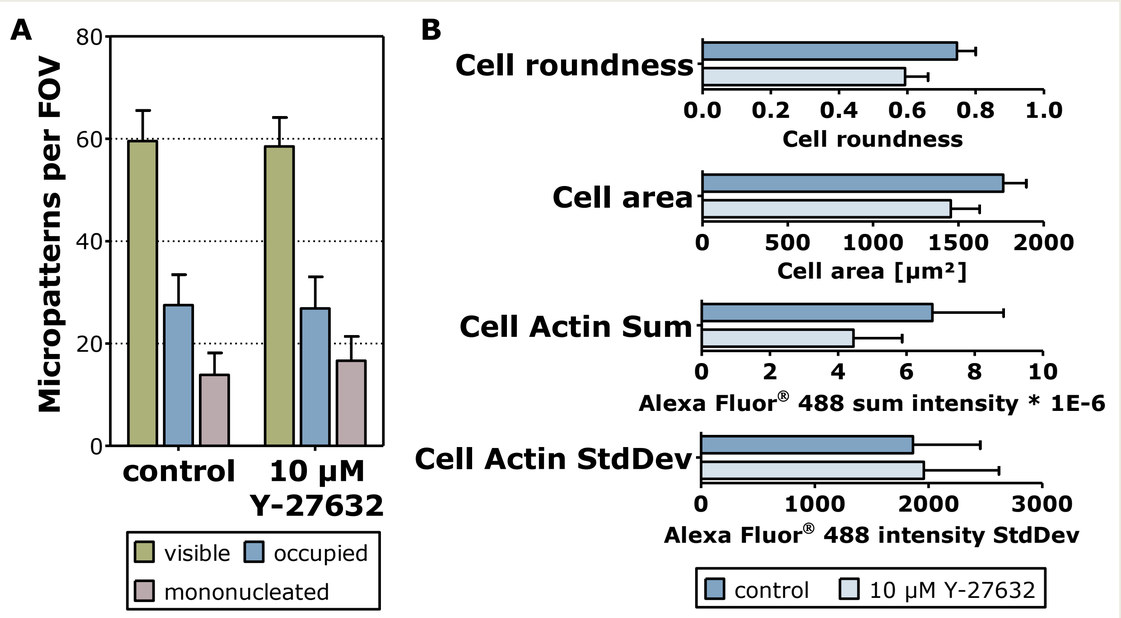

Figure 3. Evaluation of micropattern occupation and the cytoskeletal phenotype of podocytes. A) Quantification of micropattern occupation per field of view (FOV). Error bars indicate standard deviation (n=54 image fields). Per FOV we had approximately 60 fully visible micropatterns. We found roughly 27 micropatterns occupied per FOV. Of those, only 13.9 ± 1.2 in the control sample and 16.6 ± 1.3 in the ROCK inhibitor (Y-27632)-treated sample were occupied by a single cell. B) Morphology and intensity properties describing the actin cytoskeleton of untreated (control) vs. Y-27632-treated podocytes. The biggest difference between the two samples was in the 'Cell roundness'. Error bars indicate standard deviation (n=749 cells (control) and n=898 cells (Y-27632)).

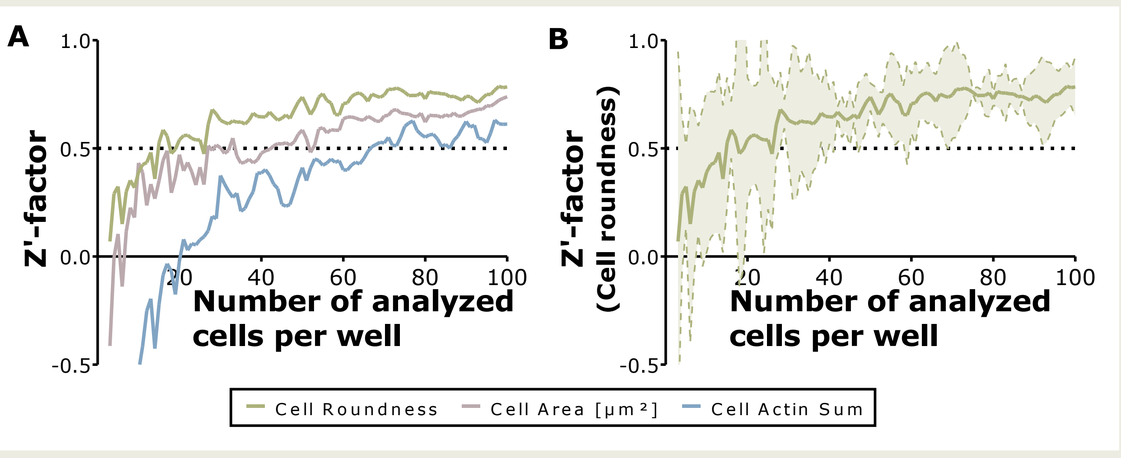

Figure 4. Statistical analysis of assay quality using the Z' factor as a function of the contributing cells per well. A varying number of cells were grouped into wells *in silico* and the Z' factor calculated. A) Comparison of the 3 best readouts obtained. The Z' factor increases with the number of contributing cells per well. B) Z' factor of the property 'Cell roundness' plotted against the number of analyzed cells per well. The grey area indicates the 95% confidence interval. The variation in the Z' factor decreases with an increasing number of analyzed cells since the sampled cells reflect the real distribution of triangular and L-shaped podocytes more reliably. The analysis revealed that at least 40 cells per well should be analyzed in order to robustly obtain an excellent Z' factor. Due to the large FOV of the Operetta system, only 4 fields have to be acquired for a reliable analysis.

4 Phenotype visualization via an average cell image

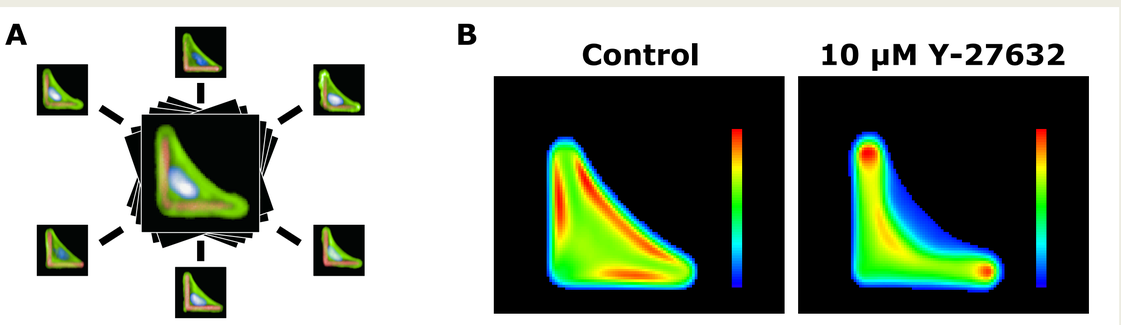

Figure 5. Calculation of an average cell for each treatment phenotype using the Acapella® High Content Imaging and Analysis Software (PerkinElmer). A) Individual micropatterns were excised from the original images. The obtained cell images were then superimposed based on the fluorescent micropatterns. B) False-color images of the average cells for both phenotypes obtained from 665 control cells and 705 Y-27632-treated cells. The average intensity of the actin staining is reflected in the color code, from red (strong signal) to blue (weak signal).

5 Summary

Here, we present a HCS assay for nephrotoxicity based on CYTOO micropatterns. Podocytes grown on micropatterns are challenged to form complex cytoskeletal structures similar to the *in vivo* situation. The low cell-to-cell variation allows for the quantification of cytoskeletal alterations in the podocyte. This is precluded by heterogeneity when using standard cell culture dishes. The large FOV of the Operetta system reduces the number of image fields needed for robust assay statistics, and the building block-based analysis of the Harmony software provides an easy tool to evaluate the cellular phenotype on the CYTOO micropatterns. Furthermore, using the Acapella software we were able to calculate an average cell that allows visualization of phenotypic changes at a glance.

Mathieson, P. W. (2012): The podocyte as a target for therapies--new and old. *Nat. Rev. Nephrol.*, 8(1), 52–56.
Saleem, M. A. *et al.* (2002): A conditionally immortalized human podocyte cell line demonstrating nephrin and podocin expression. *JASN*, 13(3), 630–638.
Wang, L. *et al.* (2012): Mechanisms of the proteinuria induced by Rho GTPases. *Kidney Int.*, 81(11), 1075–1085.

PerkinElmer, Inc., 940 Winter Street, Waltham, MA USA (800) 762-4000 or (+1) 203 925-4602 www.perkinelmer.com/lifesciences
Evotec AG, Manfred Eigen Campus, Essener Bogen 7, 22419 Hamburg, Germany www.evotec.com